TRANSIENT BEHAVIOR OF THE C-L ACID FOR THERMAL ENERGY STORAGE

Maria Natalia Roxas-Dimaano [1] and Takayuki Watanabe [2]

[1] Faculty of Engineering / Research Center for the Natural Sciences
University of Santo Tomas, Espana, Manila 1008 Philippines
Tel.: (632) 731-3101 local 4041; Fax: (632) 731-4031
E-mail: **mdimaano@ustcc.ust.edu.ph**

[2] Research Laboratory for Nuclear Reactors
Tokyo Institute of Technology
2-12-1 O-okayama, Meguro-ku, Tokyo 152-8550 Japan
Tel.: (632) 731-3101 local 4041; Fax: (632) 731-4031
E-mail: **watanabe@nr.titech.ac.jp**

A numerical analysis is made on the C-L acid that is encapsulated in a single vertical tube. The solution is facilitated by a mathematical model employing the method of finite difference for the time-dependent non-linear behavior analysis of the C-L acid on its melting and solidification. The solutions that are carried out include the existence of a moving interface between the solid and liquid phases during phase transition. The analysis and presentation of results are implied in terms of melting and the same analysis and results similarly apply to solidification with slight restructuring. The radial temperature history and distribution as well as the rates of melting and solidification results performed from the melting and solidification experiments are verified with the model. In the model, conduction constitutes the major heat transfer mechanism yielding results that are generally in better agreement in the solid phase.

Keywords: C-L acid, thermal energy storage, moving interface, heat transfer, latent heat, phase change materials

1.0 INTRODUCTION

Recent experimental studies on the melting characteristics of the fatty acid binary mixture of capric acid and lauric acid (C-L acid) indicated its potential for latent heat thermal energy storage system (Dimaano and Escoto, 1998; Dimaano and Watanabe, 2002). The primary objective of elucidating its capacity for cool storage either for air conditioning or process cooling systems necessitates an extensive analysis of its thermal characteristics. A numerical analysis on the C-L acid's instantaneous temperature distribution, heat transfer rate, and thermal storage capacity provides an effective approach to validate on its experimentally obtained information. It also provides the physical understanding of the phenomena involved in phase transitions of phase change materials (PCMs) notwithstanding the enhancement of computational capabilities appropriate to the system.

A good number of works on the numerical solution of the rate of solid to liquid phase change during a unidirectional heat transfer involving finite geometries has been

presented. One effective method is numerical integration of which the finite difference method is particularly useful [Murray and Landis, 1959; Jaluria and Torrance, 1986). Attempts have been carried out as solved by Neumann (Carlslaw and Jaeger, 1959) employing the Fourier equation in both solid and liquid phases with the established initial and boundary conditions. Previous solutions have involved heat flow with conduction as the sole transport mechanism in both solid and liquid phases disregarding the presence of convection. The inward melting or solidification of a PCM contained in a vertical tube is significantly affected by fluid motion in the liquid melt. As melting proceeds, the liquid phase has considerable lower thermal conductivities than in the solid phase. With the presence of a melted layer, heat resistance is prevented by the onset of the convective fluid motion (Bareiss and Beer, 1980, Sparrow and Broadbent, 1982). Aside from this, since the fatty acid PCM mixture has an apparent melting band-width and a non-uniform temperature during phase transition, natural convection has a role to play (Sparrow *et al.*, 1977; Farid and Mohammed, 1987). Since natural convection normally exists during the melt, its significant effect must be considered. Thus, aside from the presence of solid and liquid phases, the moving interface or boundary between them is also included in the analysis. In order to provide a better understanding of the phase change process in the C-L acid and its mixtures, computational studies are conducted for comparison with the experimental data.

2.0 NUMERICAL ANALYSIS

The PCM is placed inside a vertically cylindrical tube with hot or cold water flowing parallel to it as shown in **Figure 1**. The radial temperature and density distribution in the PCM tube are assumed to be axisymmetric representing the two-dimensional heat transfer by a one-dimensional model. The analysis takes into account the conduction-based treatment of the solid and liquid phases as well as the natural convection induced by temperature difference in the liquid melt.

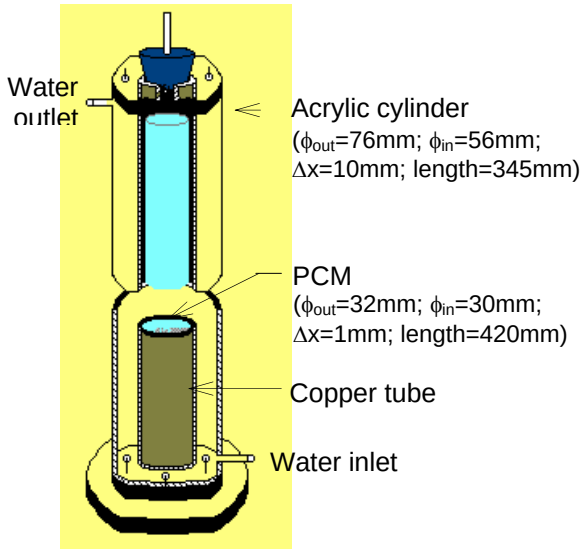

Figure 1: Schematic diagram of the PCM storage capsule.

2.1 Governing Equations

2.1.1 Energy Balance Equation

In the analysis, the mathematical model for phase change of the fatty acid PCM mixture is derived under the following assumptions:

1. The PCM behaves ideally without supercooling and property degradation.
2. The phase change of the PCM is assumed to undergo isothermal phase change.
3. The thermal resistance across the insulated cylindrical wall is assumed negligible.
4. Axial conduction in the PCM is negligible.

The system involves a non-linear transient heat conduction governed by a time dependent, one dimensional energy equation inside the cylindrical storage capsule expressed in terms of enthalpy, *H*, as

$$\rho \cdot \frac{\partial H}{\partial t} = \frac{1}{r} \cdot \left[\frac{\partial}{\partial r} \cdot \left(k \cdot \frac{r}{c_p} \cdot \frac{\partial H}{\partial r} \right) \right] \qquad (1)$$

where *r* is the interface location. The thermophysical properties are based on the prevailing solid phase, phase transition and liquid phase of the PCMs. The basic enthalpy equation in eq. (1) can be modified to give the

radial temperature distribution in the different phases of the PCM in a vertical cylinder.

The simplifying assumptions are made as follows:

1. The thermophysical properties in terms of the thermal conductivities and densities are different for the solid and liquid phases but remain constant in their corresponding solid and liquid phase domains.
2. The melt is always at its fusion temperature and that there exists at all times a sharply defined line of division indicative of the melting front between the solid and the liquid.
3. The density and specific heat during phase transition are taken on the averaged values of the liquid and solid phases.

Corresponding to the thermophysical properties in their respective domains the following simplifications are applied accordingly to a one-dimensional heat conduction approach.

For the solid phase:

$$\partial H = \rho_S \times c_{p-S} \times \partial T \qquad (2)$$

For the liquid phase:

$$\partial H = \rho_L \times c_{p-L} \times \partial T \qquad (3)$$

A different treatment is made when phase transition occurs when the sharpest variation in the thermal properties occurs. The effect of natural convection is considered during phase transition using the effective thermal conductivity, k_e, in the melted layer during phase transition that also includes the downward melting effect over the whole axial length of the vertical PCM containment.

At the solid to liquid interface, the governing equation is

$$\partial H = \rho_{ave} \times L_f \times \partial \alpha \qquad (4)$$

The melt fraction (α) is considered as the latent heat (L_f) is absorbed during melting. Phase transition is achieved as soon as the total latent heat of fusion is completed with the melt fraction equivalent to 1.0. All the heat supplied to the control volume that experiences phase transition is used for changing the amount of latent heat content of that control volume. Liquid fractions are updated from the temperature field. Although the phase transition occurs at a constant temperature, a temperature bandwidth of 0.1°C is considered for convenience in the computational analysis. A "mushy region" is established as a mixture of solid and liquid with the thermodynamic and transport properties assumed to be the arithmetic mean of the two phases.

2.2 Geometry and Boundary Conditions

2.2.1 Initial Conditions

The initial temperature of the PCM is assumed to be uniform throughout the radial positions from the center to the wall. For the initial condition, the radial temperature distribution is as follows:

$$T(r,0)=35.0°C \qquad 0 \le r \le R$$

for the melting process and

$$T(r,0)=2.0°C \qquad 0 \le r \le R$$

for the solidification process.

2.2.2 Boundary Conditions

The boundary conditions of the first kind are chosen because of experimental convenience. There are two boundary conditions considered. One boundary condition to be satisfied is its outer temperature between the water and the solid interface. Implicitly, the PCM tube wall does not go through a step change in its temperature. That is

$$T = T_w + (T_w + T_i)\exp(at) \quad \text{at } r = r_{wall} \ . \qquad (5)$$

The exponential change is considered with the value of a evaluated from the experimental measurements.
For the center PCM temperature,

$$\frac{\partial T}{\partial r} = 0 \quad \text{at} \quad r = 0. \qquad (6)$$

2.3 Thermophysical Properties

The thermophysical properties of the liquid and solid phases of the PCM mixture are different but are independent of temperature. The values respective of the solid and liquid properties of the PCMs are indicated in Table 1. The liquid and solid densities of the C-L acid with the component additives are determined considering the compositions in the mixture. Comparing the solid and liquid densities and taking the individual variations with temperature, the difference is small. Thus, taking the averaged value of the C-L acid melt during phase transition may be regarded as valid.

The liquid specific heat of the PCM mixture is determined using the Chueh Swanson group contribution method (Reid *et al.*, 1987) having proposed values of different molecular group contributions at 20°C. This method is considered accurate as errors rarely exceed 2 to 3 % from the experimental value. For the solid specific heat of the mixture, DSC derived results are considered. The variation of the specific heat of C-L acid with temperature just before it melts is very small. Thus, the averaged value of the solid and liquid specific heats is considered for the specific heat during its phase transition.

The melting points and heats of fusion of the eutectic mixture of C-L acid as well as the C-L acid in combination with the component additives are taken from the DSC analysis.

2.4 Transport Properties

2.4.1 Viscosity

The viscosity of the liquid mixture of the C-L acid is estimated employing the Grunberg and Nissan method (Reid *et al.*, 1987) employing the following relation

$$\ln \mu_m = \sum_i X_i \mu_i + \sum_i \sum_j X_i X_j G_{ij} \quad i \neq j \qquad (7)$$

For binary mixture,

$$\ln \mu_m = X_1 \ln \mu_1 + X_2 \ln \mu_2 + X_1 X_2 G_{12} \qquad (8)$$

where X = liquid mole fraction
G_{ij} = interaction parameter which is a function of the components i and j

2.4.2 Effective Thermal Conductivity

Considering an isothermal wall surface applied to vertical cylinders, the empirical correlation between the Nusselt number and the Rayleigh number (Farid, 1989) based on the PCM height and the temperature difference between the PCM surface and its melting point provides a relation to compute for the effective thermal conductivity per unit of cell as

$$k_e = k_L \times 0.28 \times Ra^{0.25} \times \left(\frac{\delta}{R} \right) \qquad (9)$$

As time proceeds, k_e increases during melting and decreases during solidification. This aids in the evaluation of natural convection in the PCM melt.

2.5 Taylor Series Approach on Numerical Development

Employing the Taylor Series approach, the following approximations employing the two dimensional grid regions for the first and second derivatives are as follows:

$$\frac{\alpha^2 T}{\partial r^2} = \frac{T_{i+1} + T_{i-1} - 2T_i}{\Delta r^2} \qquad (10)$$

$$\frac{\partial T}{\partial r} = \frac{T_{i+1} - T_{i-1}}{2\Delta r} \qquad (11)$$

$$\frac{\partial T}{\partial t} = \frac{T_i^{j+1} - T_i^{j}}{\Delta t} \qquad (12)$$

Substituting these approximations into eq. (1) provides the working equation employing the forward time central space (FTCS) explicit method

$$T_{i,j+1} = T_{i-1,j} \times \gamma + T_{i,j} \times \left[1 - \frac{\gamma}{r} \times (\Delta r + 2r) \right] + T_{i-1,j} \times \left[\frac{\gamma}{r} \times (\Delta r + r) \right] \qquad (13)$$

where γ is the grid Fourier number obtained from

$$\gamma = \frac{\alpha_e \times \Delta t}{\Delta r^2} \quad . \qquad (14)$$

The grid Fourier number must be less than or equal to 0.5 for the numerical scheme to be stable. It is safe to set γ lesser than 0.1 to minimize truncation error and thus maintain convergence and stability (Carnahan *et al.*, 1969). Farid *et al.* (1989) successfully used this approach.

The problems considered here are those of the inward melting and solidification of a cylindrical PCM of which the time required for the PCM to become totally melted or solidified and the temperature profile at that moment are determined.

3. RESULTS AND DISCUSSION

With reference to the known initial and boundary conditions, temperature – time curves were numerically computed using the approximate thermophysical properties obtained from the DSC analysis and when available, their literature values. A program employing the Digital Visual Fortran version 6.0 was used to compute for the radial temperature distribution in the PCM.

3.1. Convergence Test

Different radial and time increments were worked out in order to determine the best fitted increments for computational analysis comparison. Melting proceeds a bit slower with smaller Δts such that with the same Δr of 0.001 m, the time of melt with Δt = 1.0s is lesser than the time of melt with Δt = 0.05s. Melting proceed faster with smaller Δrs. Such that with the same Δt = 0.05 s, the time of melt with Δr = 0.0005 m is lesser than the time of melt with Δr = 0.001 m. The time it takes for higher Δt is faster within the same Δr. It takes faster melting with smaller Δr at the same Δt.

Based on the experimental results, Δr = 0.0005 m closely resembles the numerical results. It is just a matter now of choosing which Δt to use. If Δt = 0.01 s is used, the image size exceeds the maximum capacity allotted for the software application. Thus, with the other PCM samples like 50:50 CL:P, this problem will naturally occur since its melting point is very low, requiring for greater number of iterations.

3.2. Comparison with Experimental Data

Different temperatures of the working fluid taken as the wall temperatures at 30.0°C, 35.0°C, and 40.0°C were considered for the melting process and only 2.0°C for the solidification process in conformance to the experimental condition. A series of numerical tests were performed. The effect of the inlet temperature of the working fluid in the melting and solidification processes was evaluated. The correlation of the designated conditions to the timewise variation in the temperature distribution in different PCM radial positions employing the numerical model had been established. As convection takes effect from solid to liquid phase transition on to complete melting or its reverse from liquid to solid phase transition, the evaluation of the effective thermal conductivity is needed. To start with, **eq. (1)** was used with its coefficient of 0.28 and a power index of 0.25. **Figure 2** shows the comparison of the numerical radial temperature distribution with the experimental results previously monitored in different height positions of the PCM in the storage capsule with wall temperature at 35.0°C. A larger discrepancy in the numerical temperature distribution with the experimental results was obtained with 30°C of water. Incomplete melting in the 1.5 mm radius numerical results indicated the mismatch in the rate of heat transfer that is strongly influenced by the convective effect accounted from the effective thermal conductivity approximation. The temperature profile recedes with an increase in the temperature of water. Generally in all the three wall temperatures, the radial temperature best agrees in the lowest height position of 25 mm from the base of the PCM tube.

The innermost radius (1.5 mm) in the solid phase offers the best agreement depicting the stable heat transfer mechanism governed by

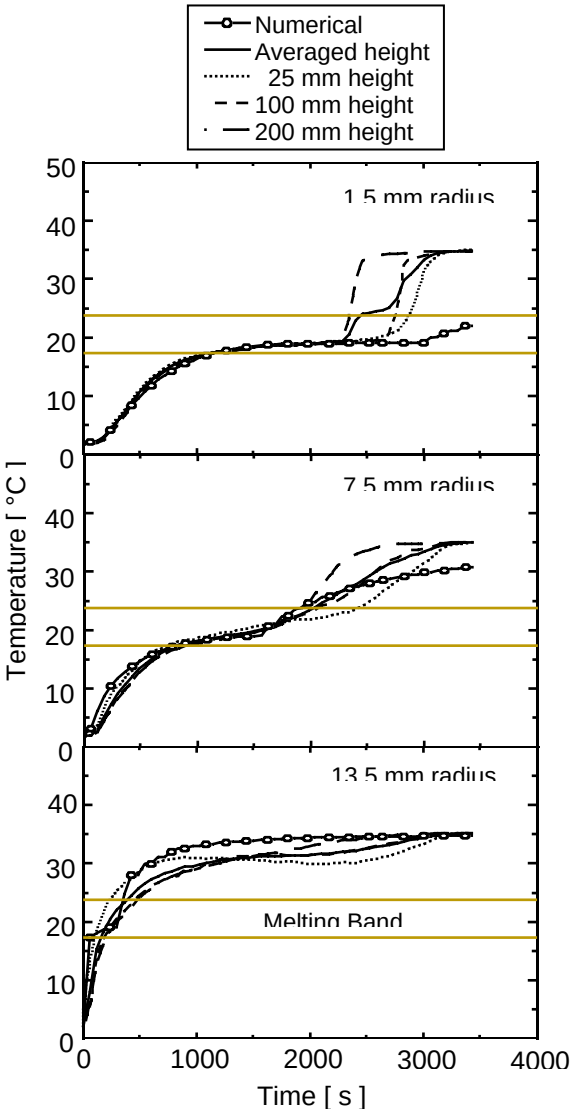

Figure 2: The radial melting temperature distribution in the C-L acid experimentally determined at different height positions employed with 35.0°C of working fluid.

conduction. With the flow patterns and temperature profiles obtained, it is inferred that convection plays a significant role during the melting process. Thus, a variation in the coefficient was made in the melting process to reproduce the experimental conditions and carry out its applicability to the current system. With the laminar flow maintained in all experiments, the power index of *Ra* was fixed at 0.25. The radius of the PCM tube was referred as the characteristic length, the length being a weak function to k_e. The coefficient influences the rate of heat transfer in the PCM. A number of numerical tests had been conducted with different coefficients. Among the different values tested, the coefficient of 0.40, as shown in **Figure 3** offered the best agreement with the radial temperature distribution in all three melting process wall temperatures. The temperature profile congruity in the innermost radial position at the lowest height position implies the certainty of a more stable heat transfer. Henceforth, the coefficient of 0.40 was thus used in the numerical analysis.

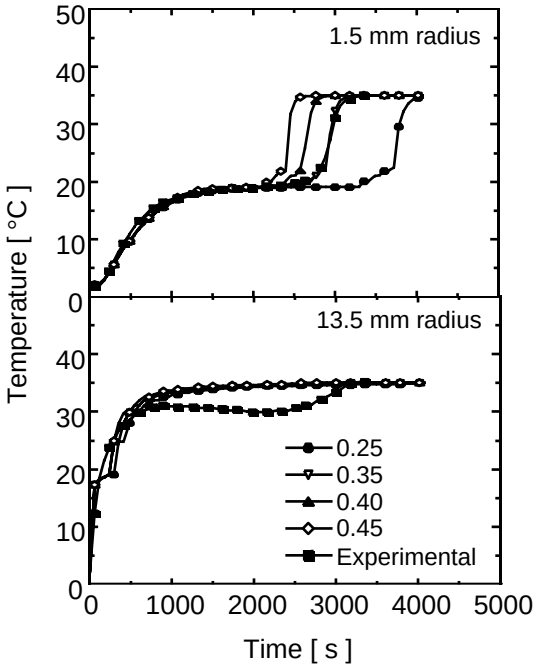

Figure 3: Radial temperature history of C-L acid obtained from different coefficients.

By comparing the results of the three working fluid temperatures, it is observed that heat transfer agrees most in the innermost radii with higher water temperatures and proceeds to decrease with decreasing fluid temperatures and height position. This is depicted from the temperature histories demonstrated in **Figures 4, 5**, and **6** correspondingly with 30.0°C, 35.0°C, and 40.0°C of working fluid temperatures in different radial positions. The numerically obtained profiles are compared with the experimental height positions taken on the average from 25 mm to 200 mm from the base of the PCM tube. The experimental temperature history in the 300 mm height position was not included to avoid end effect yields.

The lowest working fluid temperature provides the best congruency with the lowest layer and so with different height positions. The higher the temperature, the faster is the rate of heat transfer and the more stable is the convection heat transfer in the innermost radius, while it offers the least discrepancy at the 200 mm height location. Deviations exist from phase transition on to the liquid phase due to the shifting effects of convection from conduction heat transport. An apparent divergence is seen during solidification.

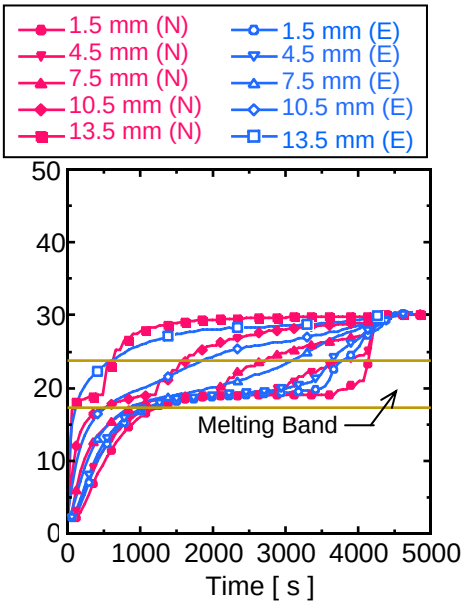

Figure 4: Comparison of numerical (N) and experimental (E) temperature history at different radial locations with 30°C of water temperature.

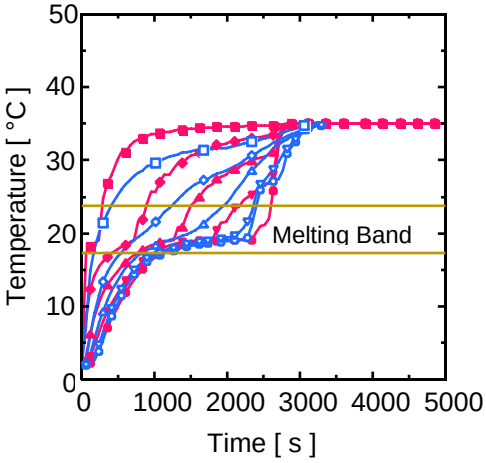

Figure 5: Comparison of numerical (N) and experimental (E) temperature history at different radial locations with 35°C of water temperature.

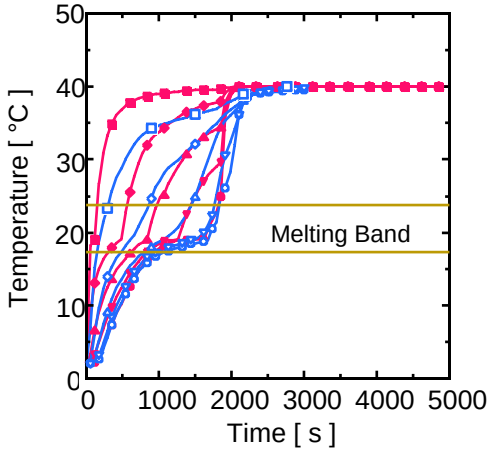

Figure 6: Comparison of numerical (N) and experimental (E) temperature history at different radial locations with 40°C of water temperature.

The effective thermal conductivity represents the combined effect of parameters composing the PCM. As the temperature difference between the working fluid and the PCM melting point increases, the strength of natural convection increases. This is depicted in **Figure 7**.

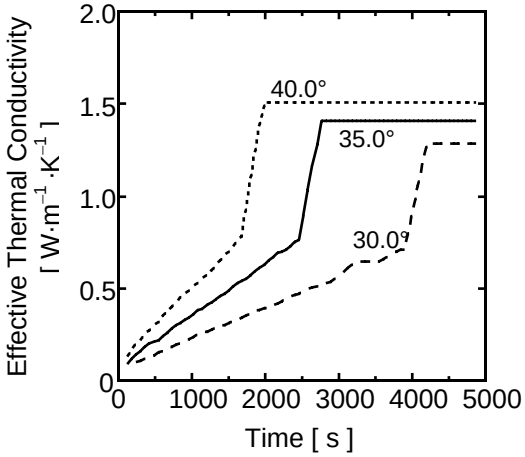

Figure 7: Melting effective thermal conductivity of C-L acid in different water temperatures.

The heat transfer conditions are different in the different layers and radial positions in the PCM. However from symmetry in the PCM tube, the same heat transfer coefficients apply as heat flows radially inward. **Figure 8** shows the convective behavior during the solid to liquid phase transition of the PCM in different working fluid temperatures.

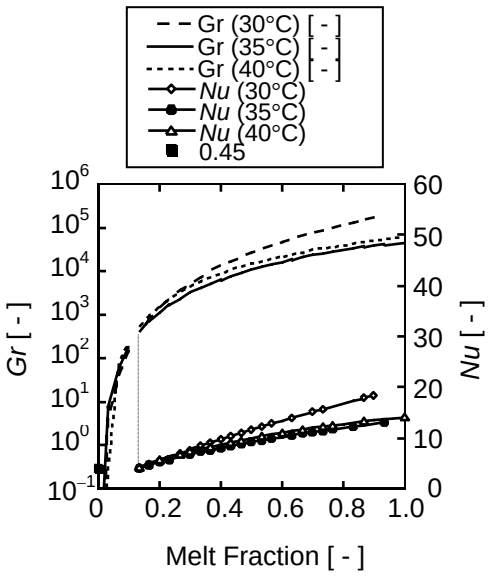

Figure 8: A plot of Grashof number and Nusselt number during C-L acid solid to liquid phase transition in different water temperatures.

The *Gr* of the PCM starts off with a very thin layer that signifies that natural convection is insignificant at the start of the melting process. The undetermined values of *Nu* from the start until melting sets in reveal the control of conduction. As melting progresses, *Gr* increase considerably and *Nu* increase linearly, indicating the taking over and eventual dominance of natural convection heat transfer. On the other hand, during solidification, *Gr* and *Nu* have initially higher values and proceed to decrease as conversely shown in **Figure 8** until complete solidification is achieved.

The temperature difference between the PCM and the working fluid greatly influences the convective strength of the PCM, as shown by the characteristic values shown in **Figures 7** and **8**. As the melting rate is actually affected by the strength of natural convection, the attainment of the designated maximum k_e directly relates to the PCM's complete melt. In **Figure 9**, the experimental melting time taken from the averaged height of 25 to 200 mm from the base of the PCM tube provides a satisfactory agreement with the numerically obtained melting time. The numerically obtained melting time is taken at the point when the maximum k_e is reached. A standard deviation of 0.0186 signifies the confidence level of the numerical model to the governing storage system.

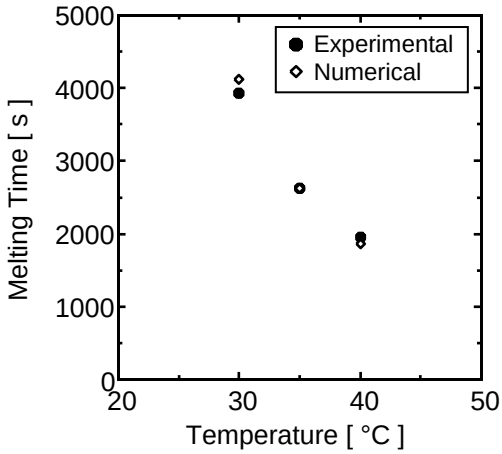

Figure 9: Melting time comparison between the numerical and experimental results.

4.2 CONCLUSION

The good agreement between the experimental and the numerical results derived from the expounded one-dimensional model provides the quantitative heat transfer data for PCM melting about a vertical cylinder. The concept proposed by Farid *et al* remains except that the coefficient of 0.40 and the radius to account for the characteristic length had been employed in this system to sustain the behavior that is characteristic and applicable to the current system. The temperature distribution and the heat transfer characteristic profiles recognize the initially brief control of heat conduction in the melt layer and the subsequent dominance of natural convection on complete melting.

Acknowledgement

The authors gratefully acknowledge the financial and moral support of the following:

- Japan Society for the Promotion of Science under the RONPAKU (Ph. D. Dissertation) Program.
- University of Santo Tomas, through Prof. Fortunato B. Sevilla III, Ph.D.
- Prof. Servillano B. Olaño, Jr., Dr. Eng. De La Salle University.

Literature Cited

Bareiss, M., and H. Beer. 1980. "Influence of natural convection on the melting process in a vertical cylindrical enclosure", *Letters in Heat and Mass Transfer***.** Vol. 7, pp. 329-338.

Brescia, F., J. Arentz, H. Meislich, and A. Turk. 1983. "Fundamentals of Chemistry", 4th ed., Academic Press, New York, pp. 277.

Carlslaw, H. S., and J. C. Jaeger. 1959. "Conduction of Heat in Solids", 2nd ed., Oxford Clarendon Press, England, pp. 282-284.

Carnahan, B., H. A. Luther, J. O. Wilkes. 1969. "Applied Numerical Methods", Wiley, New York.

Dimaano, M.N.R., and A. Escoto. 1998. "Preliminary assessment of a mixture of capric acid and lauric acids for low-temperature thermal energy storage", *ENERGY*, Vol. 23, No. 5, pp. 421-427.

Dimaano, M. N. R., and T. Watanabe. 2000. "Temperature measurement system for the mixture of capric Acid and lauric acid as a low-temperature thermal energy storage medium", *Acta Manilana*, Vol. 48, pp. 1-10.

Dimaano, M. N. R., and T. Watanabe. 2002. "Performance investigation of the capric and lauric acid mixture as latent heat energy storage for a cooling system," *Solar Energy*, Vol. 72, No. 3, pp. 205-215.

Farid, M. M., and A. K. Mohammed. 1987. "Effect of natural convection on the process of melting and solidification of paraffin wax", *Chem. Eng. Comm.*, Vol. 47, pp. 297-316.

Farid, M., Y. Kim, T. Honda, and A. Kanzawa. 1989. "The role of natural convection during melting and solidification of PCM in a vertical cylinder", *Chem. Eng. Comm.*, Vol. 84, pp. 43-60.

Holman, J.P. 1997. "Heat Transfer" 8th ed. Mc Graw Hill, Inc., USA, 346, (1997)

Jaluria, Y., and K. E. Torrance.1986. "Computational Heat Transfer", Hemisphere Publishing Corporation, Springer-Verlag, USA, pp. 117-122.

Murray, W. D., and F. Landis. 1959. "Numerical and machine solutions of transient heat conduction problems involving phase change", *Journal of Heat Transfer*, Vol. 81, pp. 106-112.

Reid, R. C., J. M. Prausnitz, and B. E. Poling. 1987. **"**The Properties of Liquids and Gases", 4th ed., Academic Press, New York.

Sparrow, E. M., and J. A. Broadbent. 1982. "Inward melting in a vertical tube which allows free expansion of the phase-change medium", *Trans. ASME Journal of Heat Transfer*, Vol. 104, pp. 309-315.

Sparrow, E. M., S. V. Patankar, and S. Ramadhyani. 1977. "Analysis of melting in the presence of natural convection in the melt region", *Trans. ASME Journal of Heat Transfer* Vol. 99, pp. 520-526.

NOMENCLATURE

c_p	specific heat of PCM [kJ kg^{-1} K^{-1}]
Gr	
H	Enthalpy [kJ kg^{-1}]
k	thermal conductivity [w m^{-1} K^{-1}]
k_e	effective thermal conductivity [w m^{-1} K^{-1}]
L	Length of capsule [m]
L_f	latent heat [kJ kg^{-1}]
r	radial position [m]
Ra	Rayleigh number
t	time [s]
T	temperature; PCM actual radial temperature [°C]
r	radius [m]
Δr	radial increment [m]
R	characteristic radius [m]
Δt	time increment [s]

Greek Symbols

α	thermal diffusivity [m^2 s^{-1}]
α_e	thermal diffusivity [m^2 s^{-1}]

δ melted layer width [m]
ρ density of PCM [kg m^{-3}]
γ grid Fourier number PCM [–]

Subscripts

$_i$ initial
$_S$ solid
$_L$ liquid
$_w$ wall or water